Title

Bioenergetic and excitotoxic determinants of cofilactin rod formation

Authors

Mai, Nguyen
Wu, Long
Uruk, Gokhan
et al.

Publication Date

2024

DOI

10.1111/jnc.16065

Peer reviewed

Received: 14 November 2023 | Revised: 12 January 2024 | Accepted: 16 January 2024

DOI: 10.1111/jnc.16065

Journal of Neurochemistry JNC The Official Journal of the International Society for Neurochemistry WILEY

ORIGINAL ARTICLE

Bioenergetic and excitotoxic determinants of cofilactin rod formation

Nguyen Mai[1,2] | Long Wu[1,2] | Gökhan Uruk[1,2] | Ebony Mocanu[1,2] | Raymond A. Swanson[1,2]

[1]Department of Neurology, University of California, San Francisco, California, USA

[2]Neurology Service, San Francisco Veterans Affairs Medical Center, San Francisco, California, USA

Correspondence
Raymond A. Swanson, Rm 482, 1700 Owens St., San Francisco, CA 94158, USA.
Email: raymond.swanson@ucsf.edu

Funding information
U.S. Department of Veterans Affairs, Grant/Award Number: 1IO1BX004884; National Institute of Neurological Disorders and Stroke, Grant/Award Number: 5R25NS070680-14

Abstract

Cofilactin rods (CARs), which are 1:1 aggregates of cofilin-1 and actin, lead to neurite loss in ischemic stroke and other disorders. The biochemical pathways driving CAR formation are well-established, but how these pathways are engaged under ischemic conditions is less clear. Brain ischemia produces both ATP depletion and glutamate excitotoxicity, both of which have been shown to drive CAR formation in other settings. Here, we show that CARs are formed in cultured neurons exposed to ischemia-like conditions: oxygen–glucose deprivation (OGD), glutamate, or oxidative stress. Of these conditions, only OGD produced significant ATP depletion, showing that ATP depletion is not required for CAR formation. Moreover, the OGD-induced CAR formation was blocked by the glutamate receptor antagonists MK-801 and kynurenic acid; the nicotinamide adenine dinucleotide phosphate (NADPH) oxidase inhibitors GSK2795039 and apocynin; as well as an ROS scavenger. The findings identify a biochemical pathway leading from OGD to CAR formation in which the glutamate release induced by energy failure leads to activation of neuronal glutamate receptors, which in turn activates NADPH oxidase to generate oxidative stress and CARs.

KEYWORDS
cofilactin rods, glutamate signaling, NADPH oxidase, neurite injury, oxidative stress, oxygen-glucose deprivation

1 | INTRODUCTION

Cofilactin rods (CARs) are intracellular aggregates of cofilin-1 and actin (Minamide et al., 2023; Yahara et al., 1996). CAR formation in neurons is increasingly recognized as a pathogenic event that leads to degeneration of neurites (axons and dendrites) in disorders ranging from stroke to Alzheimer's disease (Alhadidi et al., 2016; Alsegiani & Shah, 2020; Bahader et al., 2023; Bamburg et al., 2010; Bamburg & Bernstein, 2016; Shu et al., 2019; Won et al., 2018). CARs are formed by a biochemical pathway that involves dephosphorylation/activation of cofilin-1 and subsequent formation of disulfide linkages between neighboring cofilin-1 molecules. The upstream triggers for CAR formation include oxidative stress and ATP depletion (Ashworth et al., 2003; Huang et al., 2008; Shu et al., 2019), but it remains uncertain which of these triggers drives CAR formation under conditions of brain ischemia.

Cofilin-1 is a member of the actin depolymerizing factor-cofilin family. Its role in cellular homeostasis involves regulating dynamic actin turnover by destabilizing actin filaments to generate new monomers for polymerization and by severing actin filaments to create free barbed ends used for actin polymerization (Carlier et al., 1997; Ichetovkin et al., 2002). Cofilin-1 also binds cooperatively along F-actin to generate stable cofilactin filaments, which

Abbreviations: 2-DG, 2-deoxyglucose; CAR, cofilactin rod; DAPI, 4′,6-diamidino-2-phenylindole; DIV, day in vitro; DHE, dihydroethidium; IACUC, Institutional Animal Care and Use Committees; MAP 2, microtubule-associated protein 2; NAC, N-acetyl cysteine; NADPH, nicotinamide adenine dinucleotide phosphate oxidase; NMDA, N-methyl-D-aspartate; OGD, oxygen-glucose deprivation; ROS, reactive oxygen species; RFP, red fluorescent protein.

This article is part of the special issue "Energetics and cognition in aging brain: Impact of substrates and microbiome".

serve cytoskeletal functions such as forming filopodia and facilitating cell migration (Bamburg et al., 2021; Hylton et al., 2022; Oser & Condeelis, 2009).

CAR formation requires initial activation of cofilin-1 by dephosphorylation of its serine-3 residue, 1:1 binding of cofilin-1 to actin, and subsequent formation of cofilin-1 oligomers through intermolecular disulfide bonds (Bernstein et al., 2012; Bernstein & Bamburg, 2010; Kanellos & Frame, 2016). CARs can be imaged using antibodies against cofilin-1, as rod formation condenses the normally dispersed cofilin-1 into readily observable puncta and short rod-like segments. The rods form most readily in distal processes, especially dendrites, but can also form in cell bodies (Bamburg & Bernstein, 2016). CARs are biochemically distinct from the actin stress fibers that form in endothelial cells and muscle (Shi et al., 2016).

Experimentally, CAR formation can be induced in neurons by overexpression of cofilin-1 (Jang et al., 2005). In disease states such as brain ischemia, reactive oxygen species (ROS) produced through excitotoxic and reperfusion mechanisms can promote CAR formation in two ways: by releasing slingshot protein phosphatase-1 L from its binding protein to allow dephosphorylation of the cofilin serine-3 residue (Kim et al., 2009), and by promoting intermolecular disulfide bonds between cofilin-1 cysteines 39 and 147 (Bamburg & Bernstein, 2016; Bernstein et al., 2012; Bernstein & Bamburg, 2010). In addition, ATP depletion can promote CAR formation by increasing ADP–actin levels and by activating a different cofilin phosphatase, chronophin (Huang et al., 2008). Our goal here was to determine whether ATP depletion specifically drives CAR formation and neurite injury, or whether these effects are instead mediated by other factors such as glutamate excitotoxity and oxidative stress.

Oxygen–glucose deprivation (OGD) is a widely used cell culture model of brain ischemia as it produces ATP depletion and, in mature neurons, also leads to glutamate excitotoxicity (Buisson & Choi, 1995; Fujimoto et al., 2004; Won et al., 2018). A prior study using this model suggested that ATP depletion was a trigger for CAR formation under OGD conditions, but given the young age of the neurons used in that study (Minamide et al., 2000), the role of the excitotoxic/oxidative stress pathway may have been underestimated. Other investigators have found that neurons are more sensitive to glutamatergic signaling after day in vitro (DIV) 13 (Choi et al., 1987), and here we evaluated CAR formation in 14- to 17-day-old cortical neuron cultures. Our results show that the CAR formation induced by OGD in these cultures can be blocked by glutamate receptor antagonists, nicotinamide adenine dinucleotide phosphate oxidase (NADPH) oxidase inhibitors, and an ROS scavenger, thereby establishing a biochemical pathway leading from energy failure to CAR formation in neurons.

2 | MATERIALS AND METHODS

2.1 | Animals

Studies were approved by the Institutional Animal Care and Use Committees (IACUC) at the San Francisco Veterans Affairs Medical Center and were performed in accordance with the National Institutes of Health Guide for the Care and Use of Laboratory Animals. Work was performed in accordance with a protocol approved by the San Francisco Veterans Affairs Health System IACUC (#20-009). Wild-type C57Bl/6 mice (Jackson Laboratory, Bar Harbor, ME) were used for the procurement of embryonic cortical neurons. Mice were paired for timed pregnancies, and a total of 16 dams were euthanized when embryos reached gestational age E16-18. Dams were euthanized by cervical dislocation under isoflurane anesthesia. Embryos were retrieved, placed on ice, and immediately decapitated for neuron isolation. Five embryos were harvested from each dam (80 embryos total).

2.2 | Neuron culture and oxidative stress exposures

Cortical neurons were dissociated from E16-18 mouse embryos and cultured in Neurobasal-A medium (Gibco #10888022, Grand Island, NY) containing 5 mM glucose (Gibco #A2494001), 230 μM pyruvate (Gibco #11360070), 0.5 mM GlutaMAX (Gibco #35050061), and B-27 supplements (Gibco #17504044). Neurons were plated on poly-D-lysine-coated 8-well chamber slides at 15000 cells/well for live cell imaging, on glass coverslips in 24-well plates at 150000 cells/well for drug treatment experiments, or in 96-well plates at 30000 cells/well for ATP assays. Cells were maintained at 37°C in 5% CO_2 and balance air and underwent half media changes every 3 to 4 days. Neurons for live cell imaging were used at DIV 3, prior to extensive branching, to allow better visualization of individual neurites. For drug experiments, neurons were used at DIV 14–17 to allow for the expression of N-methyl-D-aspartate (NMDA) and other glutamate receptors and for the formation of robust synaptic contacts (Suh et al., 2008). These culture conditions have been previously shown by our lab to yield >99% neurons (Suh et al., 2008). No randomization was performed to allocate culture wells in the study. Prior to each experiment, wells were visually confirmed to be of equal confluence.

Chemical OGD was initiated with three media exchanges using glucose-free Neurobasal-A medium, followed by addition of 0.5 mM 2-deoxyglucose (2-DG) and 5 mM sodium azide (NaN_3). Initial proof-of-concept experiments were conducted with 2 h of OGD. As we later found that 20 min of OGD was sufficient in causing ATP depletion as well as rod formation, later experiments were conducted with 20 min of OGD. OGD experiments were terminated without reintroduction of normal culture medium. Thirty-minute exposures to glutamate or hydrogen peroxide (H_2O_2) were performed after washing with Neurobasal-A containing 5 mM glucose.

2.3 | Inhibition of CAR formation

One hour prior to OGD, neurons were pre-treated with a phospho-cofilin-1 (pSer3) synthetic peptide (5 μg/mL; ECM Biosciences #CX1155, Versailles, KY) which targets cofilin-1 dephosphorylation

(Long et al., 2019; Shaw & Bamburg, 2017; Zhou et al., 2012). The peptide was also included in the OGD medium.

2.4 | Live cell imaging of cofilin-1 overexpression—induced CAR formation

CAR formation was induced and visualized by overexpression of cofilin-1 using a construct in which red fluorescent protein (*RFP*) was inserted into the *CFL1* gene (cofilin-1-RFP) (Addgene plasmid #50856, Watertown, MA). Neurons at DIV 3 were Lipofectamine-transfected (Thermo Fisher #18324012) with 0.25 μg plasmid/imaging chamber. Cells were photographed at 15, 21, and 27 h after transfection. The cultures were incubated with calcein green AM (10 μM, Thermo Fisher #C34852) for 30 min prior to imaging to permit visualization of intact cell bodies and processes. Non-fluorescent calcein AM crosses the cell membrane and is hydrolyzed by endogenous esterase to the fluorescent calcein green product in live cells. Calcein green is then retained in the cell but leaks out when the cell membrane becomes compromised (Gatti et al., 1998).

2.5 | ATP determinations

Fluorometric analysis of ATP content was conducted in 96-well plates using the Abcam ATP Assay Kit (Abcam #ab83355, Cambridge, UK) using ATP standards to confirm linearity. Data were collected as nmol/well and expressed relative to values obtained in control wells performed in parallel.

2.6 | Experimental procedures

Where used, drugs were added to culture media 10 min prior to the addition of glutamate or initiation of OGD. MK-801 (#M107), apocynin (#178385), and kynurenic acid (#K3375) were obtained from Millipore Sigma (St. Louis, MO); GSK2795039 (#33777) was obtained from Cayman Chemical (Ann Arbor, MI); and N-acetyl cysteine (NAC, #A15409.36) was obtained from Thermo Fisher.

Dihydroethidium (DHE) (2 μM; Thermo Fisher #D11347) was added to the medium at the beginning of OGD, glutamate, or H_2O_2 exposures and maintained for 30 min. Hoechst 10 μM (Thermo Fisher #62249) was added immediately prior to imaging to identify cell nuclei. For live imaging, Hoechst was preferred for greater cell permeability and lower toxicity compared to 4′,6-diamidino-2-phenylindole (DAPI) (Bucevičius et al., 2018). All photographs were prepared with the same microscope under identical illumination and data capture conditions. For assessments of DHE oxidation, one central, low-magnification image was taken at 2.5× magnification from each culture well. Images were analyzed using ImageJ and data presented as DHE-positive area/area of Hoechst-positive nuclei.

Antibody sources and dilutions used are presented in Table 1. For evaluation of CAR formation, cells were fixed in a 4%

TABLE 1 Antibodies and dyes used for immunofluorescence.

	1° antibody (species)/dye	Dilution/ concentration	Incubation (temperature)	Vendor	2° antibody	Dilution	Incubation (temperature)	Vendor
Fixed Cells	MAP2 (mouse)	1:500	18 h (4°C)	Thermo Fisher #MA1-25043	Goat anti-mouse Alexa Fluor 488	1:1000	1 h (20°C)	Thermo Fisher #A28175
	Cofilin-1 (rabbit)	1:500	18 h (4°C)	Cell Signaling #5175	Goat anti-rabbit Alexa Fluor 594	1:1000	1 h (20°C)	Thermo Fisher #A-11012
	DAPI	1:1000	5 min (20°C)	Thermo Fisher #D1306	n/a	-	-	-
Live Cells	DHE	2 μM	30 min (37°C)	Thermo Fisher #D11347	n/a	-	-	-
	Hoechst	10 μM	1 min (20°C)	Thermo Fisher #62249	n/a	-	-	-
	Calcein Green AM	10 μM	30 min (37°C)	Thermo Fisher #C34852	n/a	-	-	-

paraformaldehyde solution for 40 min, rinsed in 1% phosphate buffer, and then permeabilized with 100% methanol for 15 min. Coverslips were stained using rabbit anti-cofilin-1 antibody, mouse anti-microtubule-associated protein 2 (MAP2) antibody, and DAPI. MAP2 was used as a marker of neuronal processes (Dawson & Hallenbeck, 1996), and DAPI was used to identify cell nuclei (Kapuscinski, 1995). For each well, high-magnification images were taken from three arbitrary regions of comparable cell density. Images were analyzed using ImageJ and thresholded using the "Triangle" function for cofilin-1 and "Make Binary" function for MAP2 and DAPI. CAR formation was quantified as a cofilin-1-positive area normalized either to cell number or (where MAP2 was also analyzed) total neurite area. Total neurite area was defined as the combined cofilin-1-positive area and MAP2-positive area, as MAP2 immunoreactivity is attenuated in neurite regions that are cofilin-1-positive (Won et al., 2018). For neurite analyses, the MAP2 area was normalized to cell number. The experimenters taking images and analyzing the immunostaining were blinded to the treatment conditions.

2.7 | Statistical analyses

No sample size calculations were performed. In figures, the "*n*" for each study was defined as the number of independent experiments (cell preparations) or, where only a single experiment is presented, the number of technical replicates per experiment. Experiments involving quantification of CARs or neurite injury were repeated with three independent cell preparations, and CAR formation was the primary endpoint. Numerical data are expressed as means ± standard error of the mean and analyzed using one-way ANOVA followed by Dunnett's test where multiple groups were compared against a common experimental group (either glutamate or OGD). Where only two groups were compared, two-tailed *t*-tests were used. There were no normality tests or tests for outliers used. Statistical analyses were performed using Prism version 9.5.1 (Graphpad, La Jolla, CA). *p* values less than 0.05 were considered significant.

3 | RESULTS

3.1 | CAR formation can be induced by oxidative stressors and precedes neuron degeneration

We first confirmed that OGD induced CAR accumulation in neuronal cultures. The cofilin-1 aggregates formed rod-like structures, as previously reported (Won et al., 2018). Stress-induced cofilin-1-positive aggregates in neurons have previously been demonstrated to be CARs by biochemical approaches (Minamide et al., 2010), and here we additionally confirmed that the cofilin-1 aggregates were CARs by showing that their formation could be suppressed

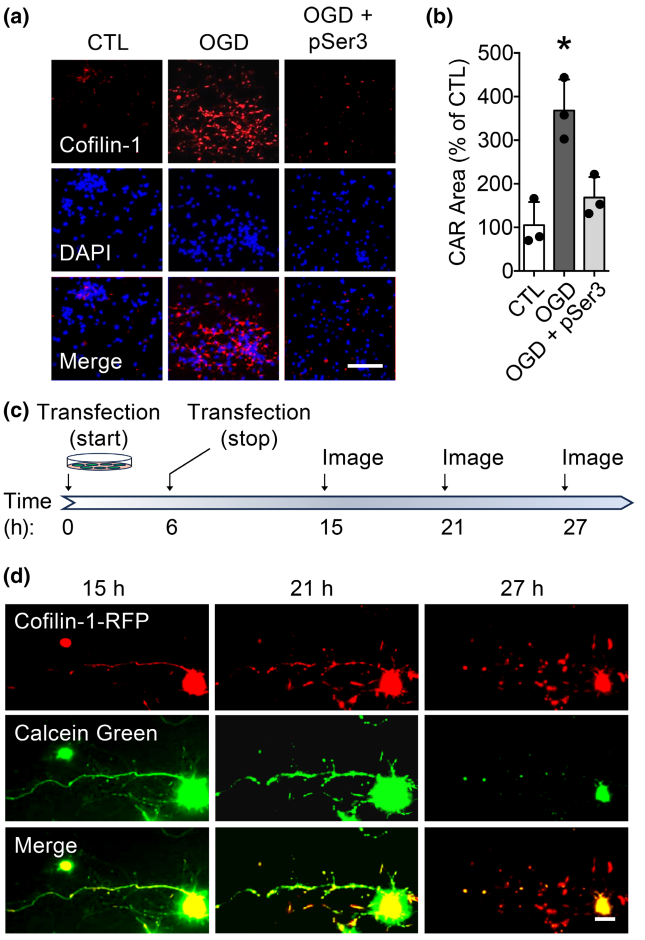

FIGURE 1 Cofilactin rods (CARs) are produced by oxidative stress and lead to neurite degeneration. (a) Primary neuronal cultures were immunostained with cofilin-1 (red), with nuclei labeled with DAPI (blue). Exposure to oxygen–glucose deprivation (OGD) for 2 h induced formation or CARs, appearing as rod-like aggregates of cofilin-1, compared to normoxic control (CTL). CAR formation was attenuated in cultures pre-incubated with the phosphoserine-3 n-terminal cofilin-1 peptide (pSer3). Scale bar = 50 μm. (b) Quantification of CAR formation defined as cofilin-1 area normalized to cell number. $N = 3$ independent cell preparations; * $p < 0.05$. Statistics: one-way ANOVA with Dunnett's multiple comparisons test. $F(2, 6) = 16.75$, $p = 0.0035$; $p = 0.0026$ (CTL vs. OGD); $p = 0.0100$ (OGD vs. OGD + pSer3). (c) Live cell imaging experimental timeline. (d) Live cell imaging of a neuron showing CAR formation induced by overexpression of a cofilin-1-RFP construct (red). The neuron is labeled with calcein green to identify cell integrity. CARs are evident within intact (green) neurites at the 21-h time point. At the 27-h time point, the neurites have degenerated, but the cell body remains. Scale bar = 5 μm. Images are representative of three experiments with similar results.

with a cofilin-1 phospho-serine-3 peptide (Figure 1a,b). An effect of CAR formation on neurite integrity was also confirmed here by artificially inducing CAR formation with cofilin-1 overexpression (Figure 1c,d; Jang et al., 2005). The overexpressed cofilin-1 construct included RFP fluorophores to permit real-time evaluation

of CAR formation, and the cultures were additionally incubated with calcein green AM before imaging. This approach also showed rod-like inclusion formation within neurites and further showed that these occur prior to neurite rupture and loss of calcein green signal.

3.2 | ATP depletion is sufficient but not necessary for CAR formation

OGD in culture, like ischemia in vivo, produces ATP depletion with glutamate release and oxidative stress as downstream events. Here, we evaluated the mechanisms of OGD, glutamate, and H_2O_2 on CAR formation using conditions previously established to generate roughly equivalent CAR densities (Figure 2a–f). Longer duration of OGD resulted in qualitatively greater CAR formation (Figure 1a depicting CARs after 2-h OGD). However, we found evidence of CARs after as little as 20 min of OGD (Figure 2a,b). We also found that OGD produced a rapid and near-complete ATP depletion (Figure 3a), whereas glutamate and H_2O_2 exposures did not (Figure 3b,c), thus confirming that ATP depletion is not necessary for neuronal CAR formation.

3.3 | Glutamate and OGD induce intracellular oxidative stress

We next sought to determine whether CAR formation in the setting of OGD was instead caused by OGD-induced oxidative stress. OGD leads to glutamate release, which in turn leads to oxidative stress by stimulating the NMDA receptor/NADPH oxidase pathways (Brennan et al., 2009; Brennan-Minnella et al., 2013). Here, we confirmed that OGD induced intracellular oxidative stress using the dihydroethidium method with H_2O_2 exposure as a positive control. These studies also confirmed that the oxidative stress induced by either glutamate (Figure 4a,c) or OGD (Figure 4b,c) could be blocked by the glutamate receptor antagonists kynurenic acid or MK-801 (Song et al., 2018; Zhen et al., 2022); by the NADPH oxidase inhibitors GSK2795039 (Hirano et al., 2015) and apocynin (Brennan et al., 2009); and by the ROS scavenger NAC (Zafarullah et al., 2003).

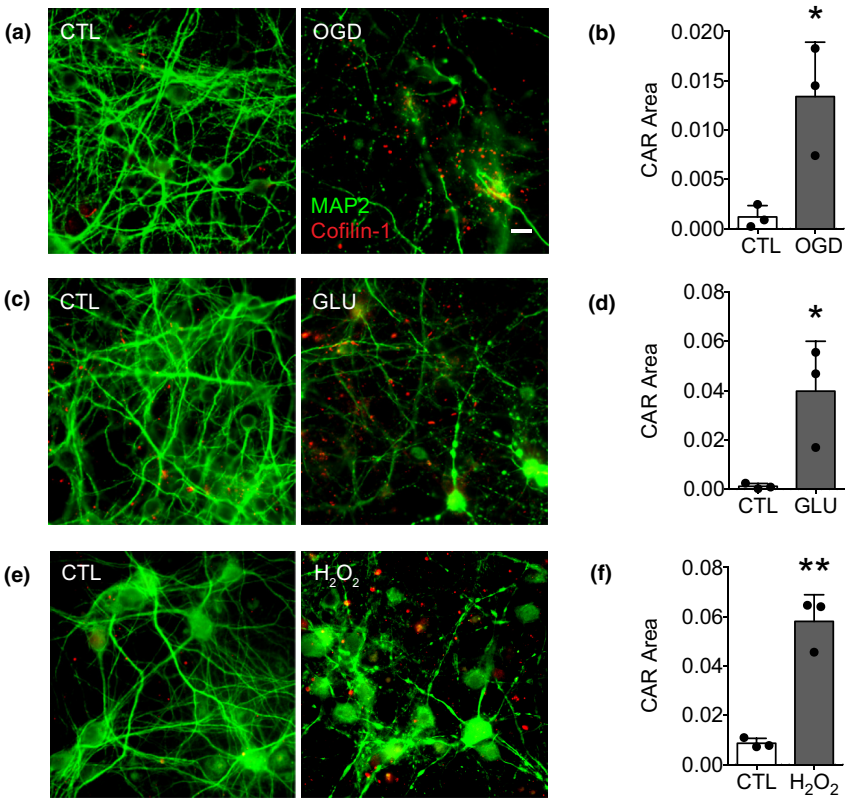

FIGURE 2 Cofilactin rod (CAR) formation is induced by exposure to oxygen–glucose deprivation (OGD), glutamate (GLU), or hydrogen peroxide versus control (CTL). Graphs and representative images depict the total area of CARs formed compared to total neurite area (MAP2 + cofilin-1) after 20 min of OGD (a, b), exposure to 30 min of glutamate 10 μM (c, d), or exposure to 30 min of H_2O_2 10 μM (e, f). Images show neurites (MAP2, green) and aggregated cofilin-1 (CARs, red) in neuronal cultures. Scale bar = 10 μm. $N = 3$ independent cell preparations; * $p < 0.05$, ** $p < 0.01$. Statistics: two-tailed t-test. CTL vs. OGD: $t(4) = 3.752$, $p = 0.0199$. CTL vs. GLU: $t(4) = 3.297$, $p = 0.0300$. CTL vs. H_2O_2: $t(4) = 7.788$, $p = 0.0015$.

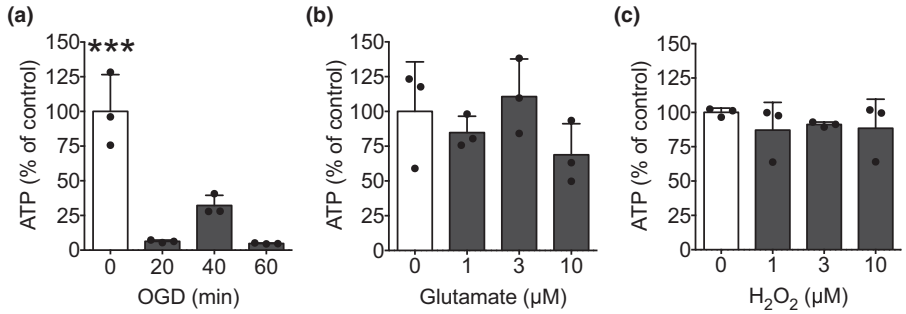

FIGURE 3 Effects of oxygen–glucose deprivation (OGD), glutamate (GLU), or hydrogen peroxide on neuronal ATP levels. (a) ATP is depleted after 20 min of chemical OGD. (b) Exposure to glutamate did not cause a reduction in ATP production after 30 min. (c) There was also no effect of H_2O_2 on ATP production after 30 min. Results are representative of two independent cell preparations with similar results. $N = 3$ wells per group; *** $p < 0.001$. Statistics: one-way ANOVA with Dunnett's multiple comparisons test. OGD: $F(3, 8) = 31.43$, $p < 0.0001$; $p < 0.0001$ (0 vs. 20 min); $p = 0.0008$ (0 vs. 40 min); $p < 0.0001$ (0 vs. 60 min). GLU: $F(3, 8) = 1.516$, $p = 0.2831$. H_2O_2: $F(3, 8) = 0.4676$, $p = 0.7130$.

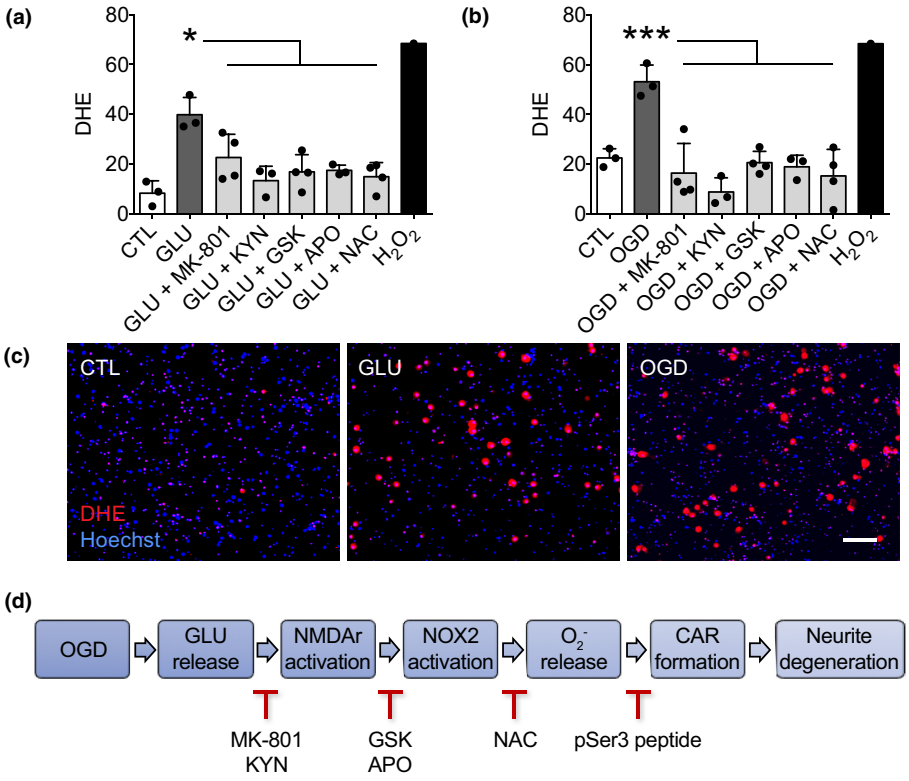

FIGURE 4 Effects of oxygen–glucose deprivation (OGD), glutamate (GLU), and drug pre-treatment on superoxide production. Exposure to either glutamate (a) or chemical OGD (b) causes the production of superoxide measured by dihydroethidium (DHE) fluorescence normalized to cell number. This is suppressed by MK-801 (100 μM), kynurenic acid (KYN, 500 μM), GSK2795039 (GSK, 200 μM), apocynin (APO, 100 μM), or N-acetyl cysteine (NAC, 2 mM). H_2O_2 100 μM treatment serves as a positive control. (c) Representative images of control (CTL), glutamate-exposed (GLU), and OGD-exposed neurons. $N = 1$ independent cell preparation with three–four wells per experimental group; * $p < 0.05$, *** $p < 0.001$. Images show DHE-positive neurons (red) and cell nuclei (Hoechst, blue). Scale bar = 100 μm. Statistics: one-way ANOVA with Dunnett's multiple comparisons test. Glutamate: $F(6, 17) = 7.411$, $p = 0.0005$; $p = 0.0001$ (GLU vs. CTL); $p = 0.0156$ (GLU vs. GLU + MK-801); $p = 0.0007$ (GLU vs. GLU + KYN); $p = 0.0012$ (GLU vs. GLU + GSK); $p = 0.0028$ (GLU vs. GLU + APO); $p = 0.0006$ (GLU vs. GLU + NAC). OGD: $F(6, 17) = 10.13$, $p < 0.0001$; $p = 0.0010$ (OGD vs. CTL); $p < 0.0001$ (OGD vs. OGD + MK-801); $p < 0.0001$ (OGD vs. OGD + KYN); $p = 0.0002$ (OGD vs. OGD + GSK); $p = 0.0003$ (OGD vs. OGD + APO); $p < 0.0001$ (OGD vs. OGD + NAC). (d) Proposed mechanism linking OGD to CAR formation.

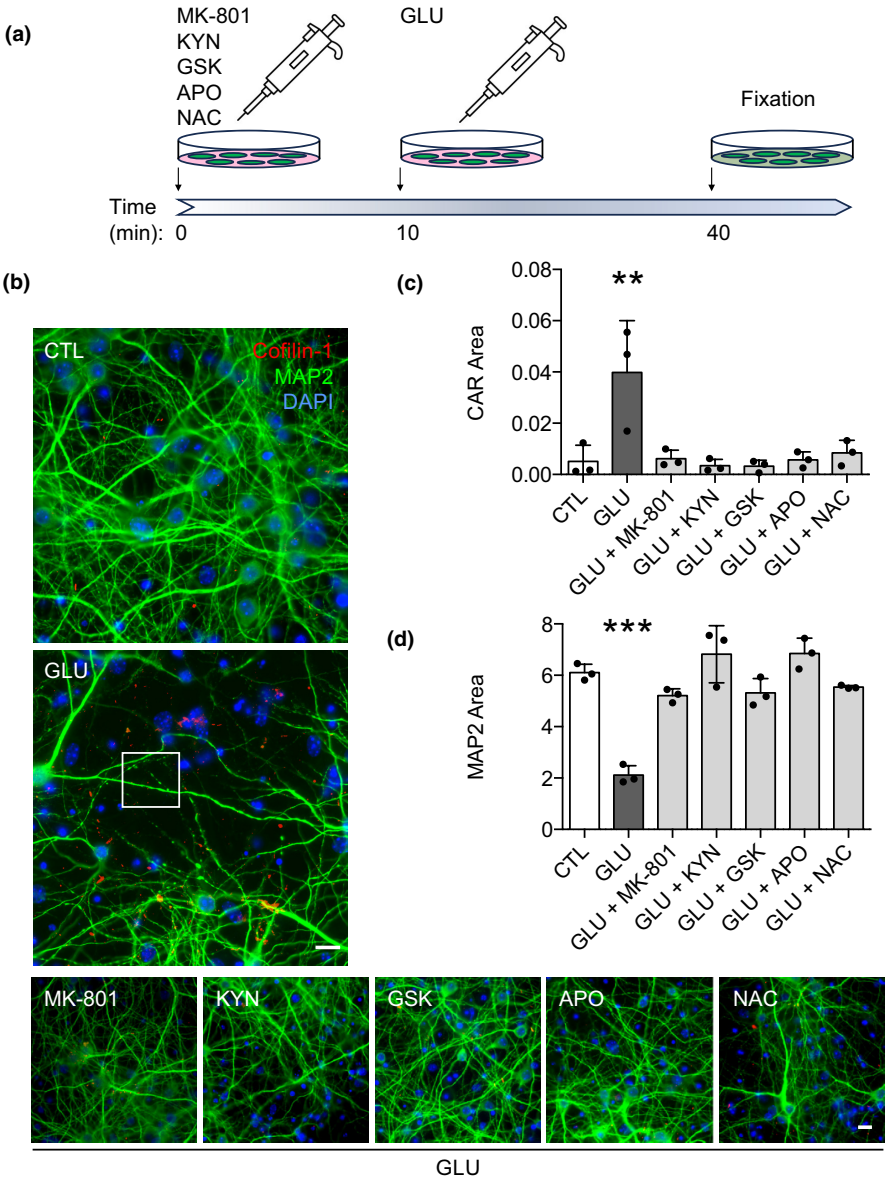

FIGURE 5 Glutamate-induced cofilactin rod (CAR) formation and neurite injury are prevented by glutamate receptor blockade, nicotinamide adenine dinucleotide phosphate (NADPH) oxidase inhibition, and ROS scavenging. (a) Experimental timeline. (b) Images show neurites (MAP2, green) and aggregated cofilin-1 (CARs, red) in neuronal cultures, with nuclei labeled with DAPI (blue). Glutamate (GLU, 10 μM) induces CAR formation, neuritic beading (example within white square), and loss of MAP2-positive neurites after 30 min. These changes are attenuated by glutamate receptor blockers MK-801 (100 μM) and kynurenic acid (KYN, 500 μM), by NADPH oxidase inhibitors apocynin (APO, 100 μM) and GSK2795039 (GSK, 200 μM), and by the ROS scavenger N-acetyl cysteine (NAC, 2 mM). Scale bars = 10 μm. (c) Quantified effects on CAR formation. $N = 3$ independent cell preparations; ** $p < 0.01$, *** $p < 0.001$. Statistics: one-way ANOVA with Dunnett's multiple comparisons test. $F(6, 14) = 24.34$, $p < 0.0001$; $p < 0.0001$ for GLU vs. all groups. (d) Quantified effect on the MAP2 area normalized to cell number. $F(6, 14) = 7.161$, $p = 0.0012$; $p = 0.0010$ (GLU vs. CTL); $p = 0.0013$ (GLU vs. GLU + MK-801); $p = 0.0007$ (GLU vs. GLU + KYN); $p = 0.0006$ (GLU vs. GLU + GSK); $p = 0.0012$ (GLU vs. GLU + APO); $p = 0.0034$ (GLU vs. GLU + NAC).

3.4 | Excitotoxicity and ATP depletion induce CAR formation and neurite injury by a common pathway

We then evaluated the effects of these agents on CAR formation induced by glutamate, which did not cause ATP depletion, and OGD, which did. Glutamate incubations produced CAR formation, loss of MAP2 immunoreactivity, and beading of MAP2-positive neurites (Figure 5a–d). These changes were prevented by the glutamate receptor antagonists, as expected, by the NADPH inhibitors, and by NAC. OGD likewise caused CAR formation, loss of MAP2 immunoreactivity, and beading of MAP2-positive neurites (Figure 6a–d). Also as observed with glutamate-treated cultures, these changes were attenuated by the glutamate receptor inhibitors, NADPH oxidase inhibitors, and NAC, thus indicating a common pathway.

4 | DISCUSSION

These results show that cortical neurons in culture form CARs when subjected to ischemia-like conditions: OGD, elevated extracellular glutamate, or oxidative stress. Of these conditions, only OGD produced significant ATP depletion, thus demonstrating that ATP depletion is not essential for CAR formation. Moreover, the OGD-induced CAR formation was blocked by both glutamate receptor antagonists and NADPH oxidase inhibitors. The findings thereby identify a biochemical pathway leading from OGD to CAR formation in which the glutamate release induced by energy failure leads to activation of neuronal glutamate receptors, which in turn activates NADPH oxidase to generate oxidative stress and CAR formation (Figure 4d).

There has been uncertainty regarding the stimuli for CAR formation and their teleological role in neurons. Under some conditions,

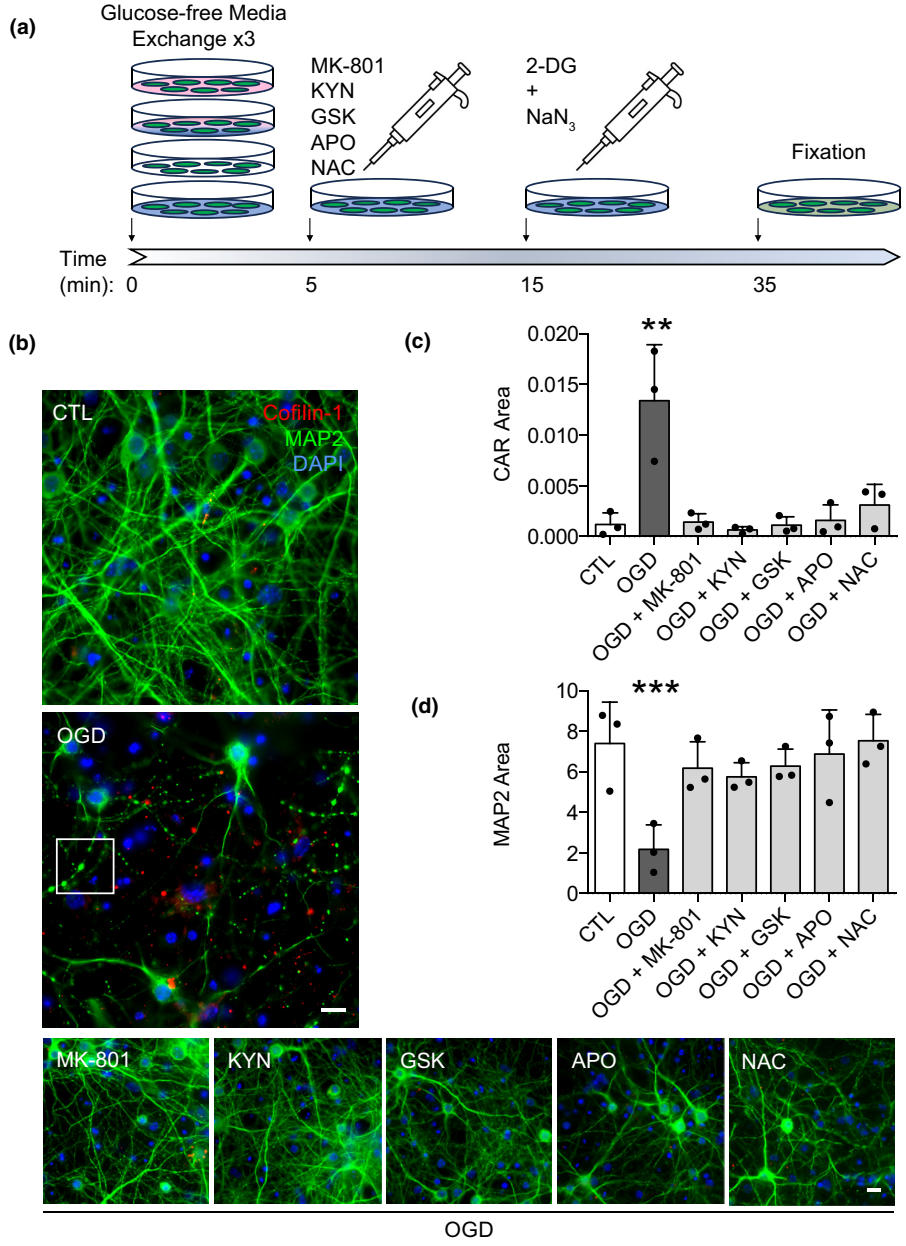

FIGURE 6 Oxygen–glucose deprivation (OGD)-induced cofilactin rod (CAR) formation and neurite injury are prevented by glutamate receptor blockade, nicotinamide adenine dinucleotide phosphate (NADPH) oxidase inhibition, and ROS scavenging. (a) Experimental timeline. (b) Images show neurites (MAP2, green) and aggregated cofilin-1 (CARs, red) in neuronal cultures, with nuclei labeled with DAPI (blue). OGD induces CAR formation, neuritic beading (example within white square), and loss of MAP2-positive neurites after 20 min. These changes are attenuated by glutamate receptor blockers MK-801 (100 μM) and kynurenic acid (KYN, 500 μM), by NADPH oxidase inhibitors apocynin (APO, 100 μM) and GSK2795039 (GSK, 200 μM), and by the ROS scavenger N-acetyl cysteine (NAC, 2 mM). Scale bars = 10 μm. (c) Quantified effects on CAR formation. $N = 3$ independent cell preparations; ** $p < 0.01$, *** $p < 0.001$. Statistics: one-way ANOVA with Dunnett's multiple comparisons test. $F(6, 14) = 10.99$, $p = 0.0001$; $p = 0.0001$ (OGD vs. CTL); $p = 0.0001$ (OGD vs. OGD + MK-801); $p < 0.0001$ (OGD vs. OGD + KYN); $p = 0.0001$ (OGD vs. OGD + GSK); $p = 0.0002$ (OGD vs. OGD + APO); $p = 0.0006$ (OGD vs. OGD + NAC). (d) Quantified effect on the MAP2 area normalized to cell number. $F(6, 14) = 4.651$, $p < 0.0084$; $p = 0.0031$ (OGD vs. CTL); $p = 0.0218$ (OGD vs. OGD + MK-801); $p = 0.0426$ (OGD vs. OGD + KYN); $p = 0.0184$ (OGD vs. OGD + GSK); $p = 0.0071$ (OGD vs. OGD + APO); $p = 0.0025$ (OGD vs. OGD + NAC).

ATP depletion has been shown to be sufficient for CAR induction (Ashworth et al., 2003; Huang et al., 2008; Minamide et al., 2000). This led to the proposal that CAR formation may generally function to spare ATP, as CAR formation interrupts all local actin-dependent processes, and these represent a large fraction of energy demand in neurites (Bernstein et al., 2006; DeWane et al., 2021). The present findings do not necessarily refute this proposal but identify a more indirect route by which energy failure leads to CAR formation in neurons.

Our results also confirm prior reports that NADPH oxidase is a primary source of oxidative stress under ischemic conditions. NADPH oxidase is a membrane-bound enzyme that utilizes NADPH to generate superoxide from molecular oxygen (Sorce &

Krause, 2009). Neurons, like most other cell types, express NADPH oxidase 2 at their plasma membranes (Keeney et al., 2022; Sorce & Krause, 2009; Tejada-Simon et al., 2005). Neuronal NADPH oxidase 2 is activated by NMDA-type glutamate receptor activation through a PKCζ-mediated pathway to release superoxide in the extracellular space (Brennan et al., 2009; Brennan-Minnella et al., 2013). Of note, neuronal NADPH oxidase can also be stimulated by prion protein binding and other factors, some of which have also been shown to also induce CAR formation (Adams et al., 1989; Dugan et al., 2009; Schneider et al., 2003; Walsh et al., 2014).

The present studies focused specifically on the biochemical events driving neuronal CAR formation under ischemic conditions, and we did not quantify long-term effects on neurite or neuronal survival in these studies. Prior studies have shown that CAR formation leads to subsequent neurite loss (Alhadidi et al., 2016; Bahader et al., 2023; Bamburg et al., 2010; Shu et al., 2019; Won et al., 2018), and the live-cell imaging study presented here in which CARs were induced by cofilin-1 overexpression further supports this contention. CAR formation has been observed after both transient and permanent focal brain ischemia (Won et al., 2018), and suppression of CAR formation has previously been shown to reduce neurite loss after brain ischemia (Shu et al., 2019).

Neurites have specialized metabolic and anatomical features arising from their need to transport signals, organelles, RNA, and proteins over long distances. These features impart unique vulnerabilities and responses to ischemic insults, such that axons and dendrites may continue to degenerate even despite survival of the parent neurons (Brown et al., 2007, 2008; Brown & Murphy, 2008). In focal ischemia, this occurs primarily in the peri-lesional tissue, where neurite loss can disrupt connections between both local and distant cells. Dendrites can regenerate, but there is variability as to the extent that regeneration recapitulates preinjury connectivity (Brown et al., 2008; Zhen et al., 2022). The mechanism by which CAR formation leads to neurite demise has not been established, but CAR formation has been shown to impair axonal and dendritic transport, drive mitochondrial fission, and induce mitochondrial depolarization (Bamburg et al., 2010; Bernstein et al., 2006; Cichon et al., 2012; Shu et al., 2019; Whiteman et al., 2009).

The energy failure/glutamate release/oxidative stress pathway shown here to induce CAR formation and neurite degeneration has previously been shown to cause neuronal death. The present findings suggest that that this same pathway underlies neurite degeneration in ischemic brain. Given that ischemic injury can cause neurite degeneration under conditions in which the parent neurons survive, this pathway might also be targeted to prevent ischemic neurite loss.

AUTHOR CONTRIBUTIONS

Nguyen Mai: Conceptualization; data curation; formal analysis; investigation; methodology; project administration; writing – original draft. **Long Wu:** Data curation; formal analysis; methodology. **Gokhan Uruk:** Data curation; formal analysis; methodology. **Ebony Mocanu:** Data curation; methodology. **Raymond A. Swanson:** Conceptualization; funding acquisition; investigation; methodology; supervision; writing – review and editing.

ACKNOWLEDGMENTS

We thank Dr. James Bamburg, Colorado State University, for helpful discussions.

All experiments were conducted in compliance with the ARRIVE guidelines.

FUNDING INFORMATION

This work was funded by the Department of Veterans Affairs grant 1IO1BX004884 and by the National Institute of Neurological Disorders and Stroke grant 5R25NS070680-14. The data that support the findings of this study are available from the corresponding author upon reasonable request.

CONFLICT OF INTEREST STATEMENT

The authors have no conflicts of interest.

PEER REVIEW

The peer review history for this article is available at https://www.webofscience.com/api/gateway/wos/peer-review/10.1111/jnc.16065.

DATA AVAILABILITY STATEMENT

The data that support the findings of this study are available from the corresponding author upon reasonable request.

ORCID

Nguyen Mai https://orcid.org/0000-0002-4738-9733

Raymond A. Swanson https://orcid.org/0000-0002-3664-5359

REFERENCES

Adams, J. H., Doyle, D., Ford, I., Gennarelli, T. A., Graham, D. I., & McLellan, D. R. (1989). Diffuse axonal injury in head injury: Definition, diagnosis and grading. *Histopathology*, *15*, 49–59.

Alhadidi, Q., Bin Sayeed, M. S., & Shah, Z. A. (2016). Cofilin as a promising therapeutic target for ischemic and hemorrhagic stroke. *Translational Stroke Research*, *7*, 33–41.

Alsegiani, A. S., & Shah, Z. A. (2020). The role of cofilin in age-related neuroinflammation. *Neural Regeneration Research*, *15*, 1451–1459.

Ashworth, S. L., Southgate, E. L., Sandoval, R. M., Meberg, P. J., Bamburg, J. R., & Molitoris, B. A. (2003). ADF/cofilin mediates Actin cytoskeletal alterations in LLC-PK cells during ATP depletion. *American Journal of Physiology. Renal Physiology*, *284*, F852–F862.

Bahader, G. A., James, A. W., Almarghalani, D. A., & Shah, Z. A. (2023). Cofilin inhibitor protects against traumatic brain injury-induced oxidative stress and neuroinflammation. *Biology (Basel)*, *12*, 630.

Bamburg, J. R., & Bernstein, B. W. (2016). Actin dynamics and cofilin-Actin rods in alzheimer disease. *Cytoskeleton (Hoboken)*, *73*, 477–497.

Bamburg, J. R., Bernstein, B. W., Davis, R. C., Flynn, K. C., Goldsbury, C., Jensen, J. R., Maloney, M. T., Marsden, I. T., Minamide, L. S., Pak, C. W., Shaw, A. E., Whiteman, I., & Wiggan, O. (2010). ADF/Cofilin-Actin rods in neurodegenerative diseases. *Current Alzheimer Research*, *7*, 241–250.

Bamburg, J. R., Minamide, L. S., Wiggan, O., Tahtamouni, L. H., & Kuhn, T. B. (2021). Cofilin and Actin dynamics: Multiple modes of regulation and their impacts in neuronal development and degeneration. *Cell*, *10*, 2726.

Bernstein, B. W., & Bamburg, J. R. (2010). ADF/cofilin: A functional node in cell biology. *Trends in Cell Biology*, *20*, 187–195.

Bernstein, B. W., Chen, H., Boyle, J. A., & Bamburg, J. R. (2006). Formation of Actin-ADF/cofilin rods transiently retards decline of mitochondrial potential and ATP in stressed neurons. *American Journal of Physiology. Cell Physiology*, *291*, C828–C839.

Bernstein, B. W., Shaw, A. E., Minamide, L. S., Pak, C. W., & Bamburg, J. R. (2012). Incorporation of cofilin into rods depends on disulfide intermolecular bonds: Implications for Actin regulation and neurodegenerative disease. *The Journal of Neuroscience*, *32*, 6670–6681.

Brennan, A. M., Suh, S. W., Won, S. J., Narasimhan, P., Kauppinen, T. M., Lee, H., Edling, Y., Chan, P. H., & Swanson, R. A. (2009). NADPH oxidase is the primary source of superoxide induced by NMDA receptor activation. *Nature Neuroscience*, *12*, 857–863.

Brennan-Minnella, A. M., Shen, Y., El-Benna, J., & Swanson, R. A. (2013). Phosphoinositide 3-kinase couples NMDA receptors to superoxide release in excitotoxic neuronal death. *Cell Death & Disease*, *4*, e580.

Brown, C. E., Li, P., Boyd, J. D., Delaney, K. R., & Murphy, T. H. (2007). Extensive turnover of dendritic spines and vascular remodeling in cortical tissues recovering from stroke. *The Journal of Neuroscience*, *27*, 4101–4109.

Brown, C. E., & Murphy, T. H. (2008). Livin' on the edge: Imaging dendritic spine turnover in the peri-infarct zone during ischemic stroke and recovery. *The Neuroscientist*, *14*, 139–146.

Brown, C. E., Wong, C., & Murphy, T. H. (2008). Rapid morphologic plasticity of peri-infarct dendritic spines after focal ischemic stroke. *Stroke*, *39*, 1286–1291.

Bucevičius, J., Lukinavičius, G., & Gerasimaitė, R. (2018). The use of Hoechst dyes for DNA staining and beyond. *Chem*, *6*, 18.

Buisson, A., & Choi, D. W. (1995). The inhibitory mGluR agonist, s-4-carboxy-3-hydroxy-phenylglycine selectively attenuates NMDA neurotoxicity and oxygen-glucose deprivation-induced neuronal death. *Neuropharmacology*, *34*, 1081–1087.

Carlier, M. F., Laurent, V., Santolini, J., Melki, R., Didry, D., Xia, G. X., Hong, Y., Chua, N. H., & Pantaloni, D. (1997). Actin depolymerizing factor (ADF/cofilin) enhances the rate of filament turnover: Implication in Actin-based motility. *The Journal of Cell Biology*, *136*, 1307–1322.

Choi, D. W., Maulucci-Gedde, M., & Kriegstein, A. R. (1987). Glutamate neurotoxicity in cortical cell culture. *The Journal of Neuroscience*, *7*, 357–368.

Cichon, J., Sun, C., Chen, B., Jiang, M., Chen, X. A., Sun, Y., Wang, Y., & Chen, G. (2012). Cofilin aggregation blocks intracellular trafficking and induces synaptic loss in hippocampal neurons. *The Journal of Biological Chemistry*, *287*, 3919–3929.

Dawson, D. A., & Hallenbeck, J. M. (1996). Acute focal ischemia-induced alterations in MAP2 immunostaining: Description of temporal changes and utilization as a marker for volumetric assessment of acute brain injury. *Journal of Cerebral Blood Flow and Metabolism*, *16*, 170–174.

DeWane, G., Salvi, A. M., & DeMali, K. A. (2021). Fueling the cytoskeleton—links between cell metabolism and Actin remodeling. *Journal of Cell Science*, *134*, jcs248385.

Dugan, L. L., Ali, S. S., Shekhtman, G., Roberts, A. J., Lucero, J., Quick, K. L., & Behrens, M. M. (2009). IL-6 mediated degeneration of forebrain GABAergic interneurons and cognitive impairment in aged mice through activation of neuronal NADPH oxidase. *PLoS One*, *4*, e5518.

Fujimoto, S., Katsuki, H., Kume, T., Kaneko, S., & Akaike, A. (2004). Mechanisms of oxygen glucose deprivation-induced glutamate release from cerebrocortical slice cultures. *Neuroscience Research*, *50*, 179–187.

Gatti, R., Belletti, S., Orlandini, G., Bussolati, O., Dall'Asta, V., & Gazzola, G. C. (1998). Comparison of Annexin V and Calcein-AM as early vital markers of apoptosis in adherent cells by confocal laser microscopy. *The Journal of Histochemistry and Cytochemistry*, *46*, 895–900.

Hirano, K., Chen, W. S., Chueng, A. L. W., Dunne, A. A., Seredenina, T., Filippova, A., Ramachandran, S., Bridges, A., Chaudry, L., Pettman, G., Allan, C., Duncan, S., Lee, K. C., Lim, J., Ma, M. T., Ong, A. B., Ye, N. Y., Nasir, S., Mulyanidewi, S., … Rutter, A. R. (2015). Discovery of GSK2795039, a novel small molecule NADPH oxidase 2 inhibitor. *Antioxidants & Redox Signaling*, *23*, 358–374.

Huang, T. Y., Minamide, L. S., Bamburg, J. R., & Bokoch, G. M. (2008). Chronophin mediates an ATP-sensing mechanism for cofilin dephosphorylation and neuronal cofilin-Actin rod formation. *Developmental Cell*, *15*, 691–703.

Hylton, R. K., Heebner, J. E., Grillo, M. A., & Swulius, M. T. (2022). Cofilactin filaments regulate filopodial structure and dynamics in neuronal growth cones. *Nature Communications*, *13*, 2439.

Ichetovkin, I., Grant, W., & Condeelis, J. (2002). Cofilin produces newly polymerized Actin filaments that are preferred for dendritic nucleation by the Arp2/3 complex. *Current Biology*, *12*, 79–84.

Jang, D.-H., Han, J.-H., Lee, S.-H., Lee, Y.-S., Park, H., Lee, S.-H., Kim, H., & Kaang, B.-K. (2005). Cofilin expression induces cofilin-Actin rod formation and disrupts synaptic structure and function in *Aplysia* synapses. *Proceedings. National Academy of Sciences. United States of America*, *102*, 16072–16077.

Kanellos, G., & Frame, M. C. (2016). Cellular functions of the ADF/cofilin family at a glance. *Journal of Cell Science*, *129*, 3211–3218.

Kapuscinski, J. (1995). DAPI: a DNA-Specific Fluorescent Probe. *Biotechnic & Histochemistry*, *70*, 220–233.

Keeney, M. T., Hoffman, E. K., Farmer, K., Bodle, C. R., Fazzari, M., Zharikov, A., Castro, S. L., Hu, X., Mortimer, A., Kofler, J. K., Cifuentes-Pagano, E., Pagano, P. J., Burton, E. A., Hastings, T. G., Greenamyre, J. T., & di Maio, R. (2022). NADPH oxidase 2 activity in Parkinson's disease. *Neurobiology of Disease*, *170*, 105754.

Kim, J.-S., Huang, T. Y., & Bokoch, G. M. (2009). Reactive oxygen species regulate a slingshot-cofilin activation pathway. *Molecular Biology of the Cell*, *20*, 2650–2660.

Long, J., Hu, Z., Xue, H., Wang, Y., Chen, J., Tang, F., Zhou, J., Liu, L., Qiu, W., Zhang, S., Ouyang, Y., Ye, Y., Xu, G., Li, L., & Zeng, Z. (2019). Vascular endothelial growth factor (VEGF) impairs the motility and immune function of human mature dendritic cells through the VEGF receptor 2-RhoA-cofilin1 pathway. *Cancer Science*, *110*, 2357–2367.

Minamide, L. S., Hylton, R., Swulius, M., & Bamburg, J. R. (2023). Visualizing cofilin-Actin filaments by immunofluorescence and CryoEM: Essential steps for observing cofilactin in cells. *Methods in Molecular Biology*, *2593*, 265–281.

Minamide, L. S., Maiti, S., Boyle, J. A., Davis, R. C., Coppinger, J. A., Bao, Y., Huang, T. Y., Yates, J., Bokoch, G. M., & Bamburg, J. R. (2010). Isolation and characterization of cytoplasmic cofilin-Actin rods. *The Journal of Biological Chemistry*, *285*, 5450–5460.

Minamide, L. S., Striegl, A. M., Boyle, J. A., Meberg, P. J., & Bamburg, J. R. (2000). Neurodegenerative stimuli induce persistent ADF/cofilin-Actin rods that disrupt distal neurite function. *Nature Cell Biology*, *2*, 628–636.

Oser, M., & Condeelis, J. (2009). The cofilin activity cycle in lamellipodia and invadopodia. *Journal of Cellular Biochemistry*, *108*, 1252–1262.

Schneider, B., Mutel, V., Pietri, M., Ermonval, M., Mouillet-Richard, S., & Kellermann, O. (2003). NADPH oxidase and extracellular regulated kinases 1/2 are targets of prion protein signaling in neuronal and nonneuronal cells. *Proceedings of the National Academy of Sciences of the United States of America*, *100*, 13326–13331.

Shaw, A. E., & Bamburg, J. R. (2017). Peptide regulation of cofilin activity in the CNS: A novel therapeutic approach for treatment of multiple neurological disorders. *Pharmacology & Therapeutics*, *175*, 17–27.

Shi, Y., Zhang, L., Pu, H., Mao, L., Hu, X., Jiang, X., Xu, N., Stetler, R. A., Zhang, F., Liu, X., Leak, R. K., Keep, R. F., Ji, X., & Chen, J. (2016). Rapid endothelial cytoskeletal reorganization enables early blood-brain barrier disruption and long-term ischaemic reperfusion brain injury. *Nature Communications*, *7*, 10523.

Shu, L., Chen, B., Chen, B., Xu, H., Wang, G., Huang, Y., Zhao, Y., Gong, H., Jiang, M., Chen, L., Liu, X., & Wang, Y. (2019). Brain ischemic insult induces cofilin rod formation leading to synaptic dysfunction in neurons. *Journal of Cerebral Blood Flow and Metabolism*, *39*, 2181–2195.

Song, X., Jensen, M. Ø., Jogini, V., Stein, R. A., Lee, C.-H., Mchaourab, H. S., Shaw, D. E., & Gouaux, E. (2018). Mechanism of NMDA receptor channel block by MK-801 and memantine. *Nature*, *556*, 515–519.

Sorce, S., & Krause, K.-H. (2009). NOX enzymes in the central nervous system: From signaling to disease. *Antioxidants & Redox Signaling*, *11*, 2481–2504.

Suh, S. W., Shin, B. S., Ma, H., Van Hoecke, M., Brennan, A. M., Yenari, M. A., & Swanson, R. A. (2008). Glucose and NADPH oxidase drive neuronal superoxide formation in stroke. *Annals of Neurology*, *64*, 654–663.

Tejada-Simon, M. V., Serrano, F., Villasana, L. E., Kanterewicz, B. I., Wu, G.-Y., Quinn, M. T., & Klann, E. (2005). Synaptic localization of a functional NADPH oxidase in the mouse hippocampus. *Molecular and Cellular Neurosciences*, *29*, 97–106.

Walsh, K. P., Minamide, L. S., Kane, S. J., Shaw, A. E., Brown, D. R., Pulford, B., Zabel, M. D., Lambeth, J. D., Kuhn, T. B., & Bamburg, J. R. (2014). Amyloid-β and proinflammatory cytokines utilize a prion protein-dependent pathway to activate NADPH oxidase and induce cofilin-Actin rods in hippocampal neurons. *PLoS One*, *9*, e95995.

Whiteman, I. T., Gervasio, O. L., Cullen, K. M., Guillemin, G. J., Jeong, E. V., Witting, P. K., Antao, S. T., Minamide, L. S., Bamburg, J. R., & Goldsbury, C. (2009). Activated Actin-depolymerizing factor/cofilin sequesters phosphorylated microtubule-associated protein during the assembly of alzheimer-like neuritic cytoskeletal striations. *The Journal of Neuroscience*, *29*, 12994–13005.

Won, S. J., Minnella, A. M., Wu, L., Eun, C. H., Rome, E., Herson, P. S., Shaw, A. E., Bamburg, J. R., & Swanson, R. A. (2018). Cofilin-Actin rod formation in neuronal processes after brain ischemia. *PLoS One*, *13*, e0198709.

Yahara, I., Aizawa, H., Moriyama, K., Iida, K., Yonezawa, N., Nishida, E., Hatanaka, H., & Inagaki, F. (1996). A role of cofilin/destrin in reorganization of Actin cytoskeleton in response to stresses and cell stimuli. *Cell Structure and Function*, *21*, 421–424.

Zafarullah, M., Li, W. Q., Sylvester, J., & Ahmad, M. (2003). Molecular mechanisms of N-acetylcysteine actions. *Cellular and Molecular Life Sciences*, *60*, 6–20.

Zhen, D., Liu, J., Zhang, X. D., & Song, Z. (2022). Kynurenic acid acts as a signaling molecule regulating energy expenditure and is closely associated with metabolic diseases. *Front Endocrinol (Lausanne)*, *13*, 847611.

Zhou, L., Jones, E. V., & Murai, K. K. (2012). Epha signaling promotes Actin-based dendritic spine remodeling through slingshot phosphatase. *The Journal of Biological Chemistry*, *287*, 9346–9359.

How to cite this article: Mai, N., Wu, L., Uruk, G., Mocanu, E., & Swanson, R. (2024). Bioenergetic and excitotoxic determinants of cofilactin rod formation. *Journal of Neurochemistry*, *00*, 1–11. https://doi.org/10.1111/jnc.16065